

This article was downloaded by:

On: 28 January 2011

Access details: *Access Details: Free Access*

Publisher *Taylor & Francis*

Informa Ltd Registered in England and Wales Registered Number: 1072954 Registered office: Mortimer House, 37-41 Mortimer Street, London W1T 3JH, UK



Physics and Chemistry of Liquids

Publication details, including instructions for authors and subscription information:

<http://www.informaworld.com/smpp/title~content=t713646857>

Vapor-liquid equilibrium, densities, and interfacial tensions for the system benzene + propan-1-ol

Andrés Mejía^a; Hugo Segura^a; Marcela Cartes^a

^a Departamento de Ingeniería Química, Universidad de Concepción POB 160-C, Concepción, Chile

To cite this Article Mejía, Andrés , Segura, Hugo and Cartes, Marcela(2008) 'Vapor-liquid equilibrium, densities, and interfacial tensions for the system benzene + propan-1-ol', *Physics and Chemistry of Liquids*, 46: 2, 175 – 190

To link to this Article: DOI: 10.1080/00319100701459350

URL: <http://dx.doi.org/10.1080/00319100701459350>

PLEASE SCROLL DOWN FOR ARTICLE

Full terms and conditions of use: <http://www.informaworld.com/terms-and-conditions-of-access.pdf>

This article may be used for research, teaching and private study purposes. Any substantial or systematic reproduction, re-distribution, re-selling, loan or sub-licensing, systematic supply or distribution in any form to anyone is expressly forbidden.

The publisher does not give any warranty express or implied or make any representation that the contents will be complete or accurate or up to date. The accuracy of any instructions, formulae and drug doses should be independently verified with primary sources. The publisher shall not be liable for any loss, actions, claims, proceedings, demand or costs or damages whatsoever or howsoever caused arising directly or indirectly in connection with or arising out of the use of this material.

Vapor–liquid equilibrium, densities, and interfacial tensions for the system benzene + propan-1-ol

ANDRÉS MEJÍA*, HUGO SEGURA and MARCELA CARTES

Departamento de Ingeniería Química, Universidad de Concepción
POB 160–C, Correo 3, Concepción, Chile

(Received 15 March 2007; in final form 18 May 2007)

Isobaric vapor–liquid equilibrium data at 50, 75, and 94 kPa have been determined for the binary system benzene + propan-1-ol, in the temperature range 320–370 K. The measurements were made in a vapor–liquid equilibrium still with circulation of both phases. Mixing volumes have been also determined from density measurements at 298.15 K and 101.3 kPa and, at the same temperature and pressure; the dependence of interfacial tension on concentration has been measured using the maximum bubble pressure technique. According to experimental results, the mixture presents positive deviation from ideal behaviour and azeotropy is present at 50, 75, and 94 kPa. The mixing volumes of the system change from negative to positive as the concentration of benzene increases, and the interfacial tensions exhibit negative deviation from the linear behaviour. The activity coefficients and boiling points of the solutions were well-correlated with the mole fraction using the Wohl, Wilson, UNIQUAC, NRTL equations and predicted by the UNIFAC group contribution method. Excess volume data and interfacial tensions were correlated using the Redlich–Kister model.

Keywords: Vapor–liquid equilibrium; Densities; Interfacial tension

1. Introduction

Following with our continuous experimental program for determining thermophysical properties of fluid mixtures [1–31], in this work we test the capability of our laboratory which has been complemented with new interfacial tensiometry installations for reproducing both phase equilibrium and interface tension data of well-characterized mixtures. The benzene + propan-1-ol mixture has been selected since, on the one hand, experimental properties have been reported in a wide range of conditions and, on the other hand, as an example of a mixture of aromatic hydrocarbon + alcohol, it presents an interesting phase behaviour where the competence between cross and self-association play an important role. Vapor–liquid equilibrium (VLE) measurements for the quoted system have been performed in a wide range of temperature and pressure conditions. In fact, isothermal VLE measurements cover the temperature range $273.15\text{ K} < T < 553.15\text{ K}$ [32–45], while isobaric VLE measurements have been performed in the

*Corresponding author. Tel.: + 56-4122023897. Fax: + 56-41224791. Email: amejia@udec.cl

range from $13 \text{ kPa} < P < 101 \text{ kPa}$ [38,46–56]. In addition, according to the available experimental evidence, the VLE of the system benzene + propan-1-ol exhibits positive deviation from ideal behaviour and azeotropy is present in all the measured temperature conditions. The VLE data also shows that, as pressure (or temperature) increases, the azeotropic concentration of the mixture impoverishes in the component characterized by the lowest heat of vaporization (in this case benzene), thus following Wrewki's azeotropic law [57].

The dependence of excess volumes (V^E) on mole fractions was determined by Munk *et al.* at 293.15 K [58], by Brown and Smith [59] and Singh *et al.* [60] at 298.15 K, by Gupta *et al.* [61] and Kumar and Reddy [62] at 303.15 K, and by Yadav *et al.* [63] at 308.15 K. According to these authors, the V^E function changes from negative to positive deviation as the concentration of benzene increases in the temperature range $293.15 \text{ K} < T < 298.15 \text{ K}$. However, this behaviour is not confirmed by the experimental results reported by Singh *et al.* [60]. At higher temperatures, the V^E data exhibit positive deviation from ideal behaviour in whole mole fraction range.

The interfacial tensions (σ) of the mixture were determined by Brown [64] at 293.15 K, by Starobinets and Starobinets [65] and by Shastri *et al.* [66] at 298.15 K. According to these experimental results, the system benzene + propan-1-ol shows negative deviation from the linear behaviour in whole mole fraction range. In addition, the data of Shastri *et al.* [66] shows a sharp stationary point of σ in the range of diluted benzene, thus suggesting azeotropic behaviour.

This work is devoted to report accurate VLE data, thus complementing the available low-pressure information at 50, 75, and 94 kPa. As a second objective, this work elucidates some gaps regarding the experimental V^E and σ behaviour by determining carefully these data at 298.15 K.

2. Experimental section

2.1. Purity of materials

Benzene (99.7 + mass%) and propan-1-ol (99.9 + mass%) were purchased from Merck. Benzene was used without further purification and propan-1-ol was dried using 3 Å molecular sieves. After these steps, gas chromatography failed to show any significant impurity. The properties and purity of the pure components, as determined by GLC, appear in table 1. The densities and refractive indexes of pure liquids were measured at 298.15 K using an Anton Paar DMA 5000 densimeter (Austria) and a Multiscale

Table 1. Mole % GLC purities (mass %), refractive index (n_D) at Na D line, densities (ρ), normal boiling points (T_b) and interfacial tensions (σ) of pure components.

Component (purity/mass%)	n_D (298.15 K)		$\rho(\text{g cm}^{-3})$ (298.15 K)		$T_b(\text{K}^{-1})$ (101.33 kPa)		$\sigma(\text{mN m}^{-1})$ (298.15 K)	
	Exptl.	Lit.	Exptl.	Lit.	Exptl.	Lit.	Exptl.	Lit.
	Benzene (99.7+)	1.49792 ^a	1.49792 ^b	0.87346 ^a	0.87360 ^b	353.24 ^a	353.24 ^b	28.30 ^a
Propan-1-ol (99.9+)	1.38333 ^a	1.38370 ^b	0.79954 ^a	0.79960 ^b	370.30 ^a	370.30 ^b	23.50 ^a	23.39 ^c

^aMeasured.

^bRiddick [67].

^cJasper [68].

Automatic Refractometer RFM 81 (Bellingham + Stanley, England), respectively. Temperature was controlled to ± 0.01 K with a thermostated bath. The uncertainties in density and refractive index measurements are $5 \times 10^{-6} \text{ g cm}^{-3}$ and $\pm 10^{-5}$, respectively. The interfacial tensions of pure fluids were measured at 298.15 K using a maximum bubble pressure tensiometer, model PC500-LV (Sensadyne, USA). The uncertainties in interfacial tension measurements are $\pm 0.1 \text{ mN m}^{-1}$. Temperature was controlled to ± 0.1 K with a thermostated bath (Cole-Palmer, USA). The experimental values of these properties and the boiling points are given in table 1 together with those given in the literature are available.

2.2. Apparatus and procedure

2.2.1. Vapor–liquid–equilibrium cell. An all-glass VLE apparatus model 601, manufactured by Fischer Labor und Verfahrenstechnik (Germany), was used in the equilibrium determinations. In this circulation-method apparatus, the mixture is heated to its boiling point by a 250 W immersion heater. The vapor–liquid mixture flows through an extended contact line (Cottrell pump) that guarantees an intense phase exchange and then enters to a separation chamber whose construction prevents an entrainment of liquid particles into the vapor phase. The separated gas and liquid phases are condensed and returned to a mixing chamber, where they are stirred by a magnetic stirrer, and returned again to the immersion heater. The temperature in the VLE still has been determined with a Systemtechnik S1224 digital temperature meter, and a Pt 100 Ω probe calibrated at the Swedish Statens Provningsanstält. The accuracy is estimated as ± 0.02 K. The total pressure of the system is controlled by a vacuum pump capable of work under vacuum up to 0.25 kPa. The pressure has been measured with a Fischer pressure transducer calibrated against an absolute mercury-in-glass manometer (22-mm diameter precision tubing with cathetometer reading), the overall accuracy is estimated as ± 0.03 kPa.

On the average, the system reaches equilibrium conditions after 2–3 h operation. Samples, taken by syringing 1.0 μL after the system had achieved equilibrium, were analyzed by gas chromatography on a Varian 3400 apparatus provided with a thermal conductivity detector and a Thermo Separation Products model SP4400 electronic integrator. The column was 3 m long and 0.3 cm in diameter, packed with SE-30. Column, injector and detector temperatures were (353.15, 423.15, 493.15) K, respectively. Good separation was achieved under these conditions, and calibration analyses were carried out to convert the peak ratio to the mass composition of the sample. The pertinent polynomial fit had a correlation coefficient R^2 better than 0.99. At least three analyses were made of each sample. Concentration measurements were accurate to better than ± 0.001 in mole fraction.

2.2.2. Density measurements. For density measurements, samples of known mass were prepared on an analytical balance (Chyo Balance Corp., Japan) with an accuracy of $\pm 10^{-4}$ g. Densities of the pure components and their mixtures were then measured using a DMA 5000 densimeter (Anton Paar, Austria) with an accuracy of $5 \times 10^{-6} \text{ g cm}^{-3}$. The density determination is based on measuring the period of oscillation of a vibrating U-shaped tube filled with the liquid sample. The temperature of the apparatus was maintained to constant within ± 0.01 K.

2.2.3. Interfacial tension measurements. A maximum bubble pressure tensiometer model PC500-LV manufactured by Sensadyne Inc. (USA), was used in interfacial tension measurements. In this equipment, two probes of different orifice radii (r_1, r_2) are immersed in a vessel that contains the liquid sample to be measured. Then an inert gas, (e.g., Nitrogen) is blown through the probes and the differential pressure (ΔP) between them is recorded. According to the Laplace's equation, ΔP and r_1, r_2 are related to the interfacial tension, σ [69,70] as:

$$\Delta P = P_1 - P_2 = 2\sigma \left(\frac{1}{r_1} - \frac{1}{r_2} \right) \quad (1)$$

where P_i is the pressure exerted by the gas flow in the probe of radius r_i . The gas flow is controlled by a sensor unit connected to a personal computer through an interface board (PCI-DAS08, Measurement Computing, USA). Besides a constant volume flow controller, this sensor unit contains a differential pressure transducer, a temperature transducer, and pressure regulator. The temperature of the sample in the vessel is measured by means of a K-type thermocouple, and maintained to constant within ± 1 K by means of a thermostatic bath (Cole-Parmer, USA).

The experimental procedure for determining interfacial tension is as follows. The mixture to be analyzed is prepared by adding appropriate volumes of each pure fluid and, then, it is degassed in an ultrasonic bath. After appropriate degasification, the concentration of the sample is measured by gas chromatography. The sample is then placed into the vessel and heated to the experimental temperature. Thereafter, an inert gas flows through the probes and the sensor unit translates the voltage signal (Δv) to a ΔP signal. The relation between Δv – ΔP is obtained by calibrating the sensor unit using two reference fluids of well-known interfacial tensions (e.g., water and ethanol, respectively). Finally, the interfacial tension is calculated according to the equation (1). Additional details concerning to the maximum bubble pressure technique have been extensively described by Adamson and Gast [69] and Rusanov and Prokhorov [70]

3. Results and discussions

3.1. Vapor–liquid equilibrium

The equilibrium temperature T , liquid-phase x and vapor-phase y mole fraction measurements at $P=50, 75$, and 94 kPa are reported in tables 2–4 and in figures 1–4, together with the activity coefficients (γ_i) that were calculated from the following equation [71]:

$$\ln \gamma_i = \ln \frac{y_i P}{x_i P_i^0} + \frac{(B_{ii} - v_i^L)(P - P_i^0)}{RT} + y_j^2 \frac{\delta_{ij} P}{RT} \quad (2)$$

where P is the total pressure and P_i^0 is the pure component vapor pressure. v_i^L is the molar liquid volume of component i , B_{ii} , and B_{jj} are the second virial coefficients of the pure gases, B_{ij} is the cross second virial coefficient, and

$$\delta_{ij} = 2B_{ij} - B_{jj} - B_{ii} \quad (3)$$

Table 2. Experimental vapor–liquid equilibrium data for benzene (1) + propan-1-ol (2) at 50.00 kPa.

$T(\text{K})$	x_1	y_1	γ_1	γ_2	$-B_{ij}(\text{cm}^3 \text{mol}^{-1})$		
					11	22	12
352.79	0.000	0.000		1.000			
349.50	0.026	0.155	3.414	0.997	992	1210	935
347.58	0.044	0.242	3.338	0.990	1006	1239	947
344.40	0.082	0.365	2.958	0.995	1030	1289	968
341.78	0.122	0.453	2.680	1.009	1051	1333	986
339.15	0.162	0.535	2.596	1.016	1072	1379	1004
336.05	0.238	0.625	2.287	1.045	1098	1436	1027
334.15	0.305	0.677	2.064	1.080	1115	1474	1041
332.82	0.359	0.708	1.914	1.133	1126	1501	1051
331.85	0.413	0.732	1.783	1.190	1135	1521	1058
330.80	0.466	0.753	1.686	1.269	1145	1543	1067
330.45	0.535	0.769	1.517	1.389	1148	1551	1069
330.15	0.590	0.792	1.431	1.439	1151	1558	1072
329.75	0.648	0.799	1.335	1.651	1154	1566	1075
329.65	0.700	0.805	1.248	1.892	1155	1569	1076
329.55	0.755	0.818	1.180	2.175	1156	1571	1076
329.45	0.811	0.833	1.123	2.602	1157	1573	1077
329.55	0.869	0.852	1.068	3.299	1156	1571	1076
329.82	0.930	0.887	1.028	4.677	1154	1565	1074
330.05	0.947	0.903	1.020	5.214	1152	1560	1073
331.96	1.000	1.000	1.000				

Table 3. Experimental vapor–liquid equilibrium data for benzene (1) + propan-1-ol (2) at 75.00 kPa.

$T(\text{K})$	x_1	y_1	γ_1	γ_2	$-B_{ij}(\text{cm}^3 \text{mol}^{-1})$		
					11	22	12
362.59	0.000	0.000		1.000			
357.75	0.045	0.216	3.151	0.995	936	1099	886
354.60	0.085	0.348	2.946	0.983	957	1139	904
352.50	0.117	0.417	2.720	0.994	971	1168	917
350.25	0.157	0.488	2.551	1.005	987	1200	931
347.90	0.205	0.550	2.368	1.037	1004	1234	945
344.52	0.305	0.635	2.036	1.119	1029	1287	967
343.40	0.356	0.667	1.903	1.157	1038	1305	975
342.45	0.411	0.694	1.764	1.217	1046	1321	981
342.02	0.480	0.722	1.594	1.278	1049	1329	984
341.83	0.540	0.743	1.467	1.346	1050	1332	986
341.32	0.588	0.755	1.393	1.464	1055	1341	989
341.10	0.644	0.770	1.305	1.612	1056	1344	991
340.95	0.699	0.783	1.229	1.807	1057	1347	992
340.85	0.756	0.797	1.161	2.094	1058	1349	992
340.85	0.811	0.814	1.105	2.478	1058	1349	992
340.90	0.869	0.837	1.058	3.135	1058	1348	992
341.42	0.930	0.878	1.020	4.256	1054	1339	989
341.75	0.947	0.897	1.013	4.666	1051	1333	986
343.80	1.000	1.000	1.000				

Table 4. Experimental vapor–liquid equilibrium data for benzene (1) + propan-1-ol (2) at 94.00 kPa.

$T(\text{K})$	x_1	y_1	γ_1	γ_2	$-B_{ij}(\text{cm}^3 \text{mol}^{-1})$		
					11	22	12
368.35	0.000	0.000		1.000			
360.45	0.083	0.316	2.902	1.009	918	1066	870
358.22	0.119	0.390	2.651	1.025	933	1093	883
356.10	0.157	0.458	2.502	1.038	947	1120	895
354.05	0.204	0.523	2.339	1.052	961	1147	907
351.08	0.295	0.605	2.037	1.117	981	1188	925
349.98	0.346	0.635	1.884	1.166	989	1203	932
349.02	0.415	0.670	1.709	1.228	996	1218	938
348.65	0.482	0.701	1.555	1.278	999	1223	941
348.20	0.507	0.711	1.521	1.324	1002	1230	943
348.28	0.532	0.719	1.463	1.351	1001	1229	943
347.90	0.596	0.740	1.358	1.475	1004	1234	945
347.75	0.644	0.754	1.289	1.590	1005	1237	946
347.65	0.699	0.768	1.212	1.783	1006	1238	947
347.55	0.756	0.785	1.149	2.052	1007	1240	948
347.55	0.812	0.803	1.095	2.429	1007	1240	948
347.75	0.869	0.829	1.048	3.023	1005	1237	946
348.40	0.929	0.876	1.016	3.944	1000	1227	942
348.40	0.929	0.876	1.016	3.944	1000	1227	942
348.65	0.946	0.896	1.013	4.283	999	1223	941
350.84	1.000	1.000	1.000				

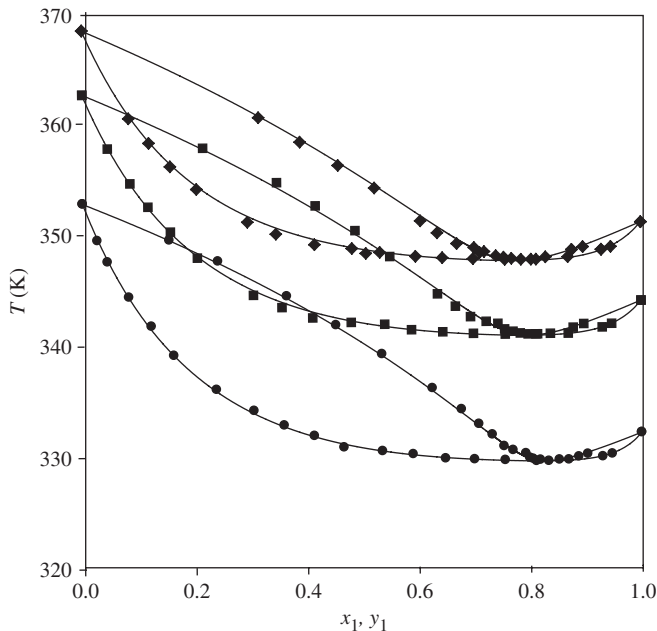


Figure 1. Boiling temperature diagram for the system benzene (1) + propan-1-ol (2). Experimental data at (●) 50.00 kPa, (■) 75.00 kPa, (◆) 94.00 kPa; (—) smoothed by the NRTL model, with parameters given in table 8.

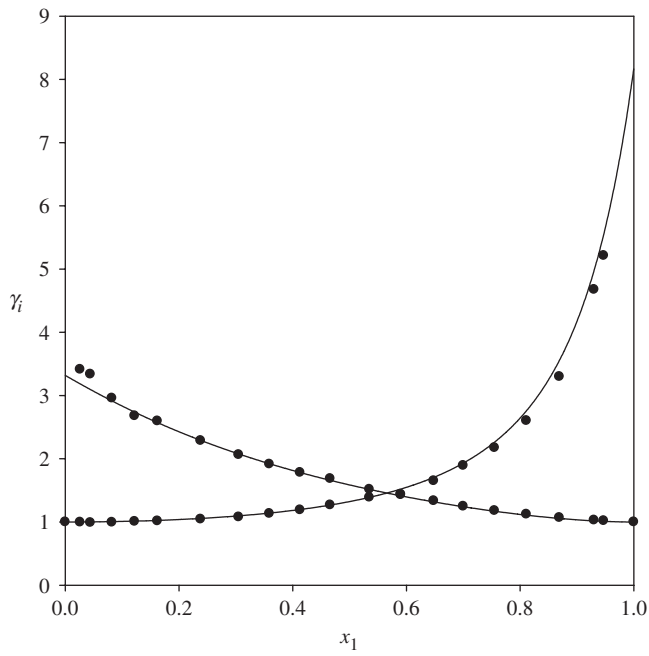


Figure 2. Activity coefficients for the system benzene (1)+ propan-1-ol (2) at 50.00 kPa. (●) Experimental data; (—) smoothed by the NRTL model, with parameters given in table 8.

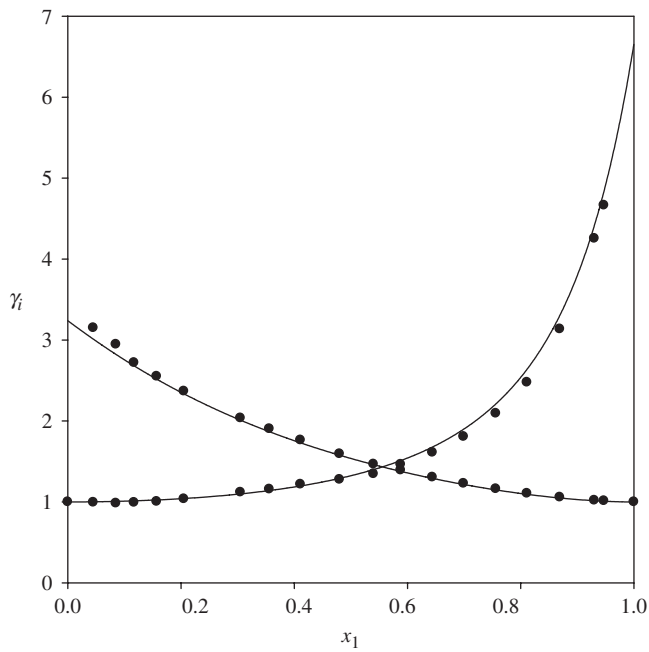


Figure 3. Activity coefficients for the system benzene (1)+ propan-1-ol (2) at 75.00 kPa. (●) Experimental data; (—) smoothed by the NRTL model, with parameters given in table 8.

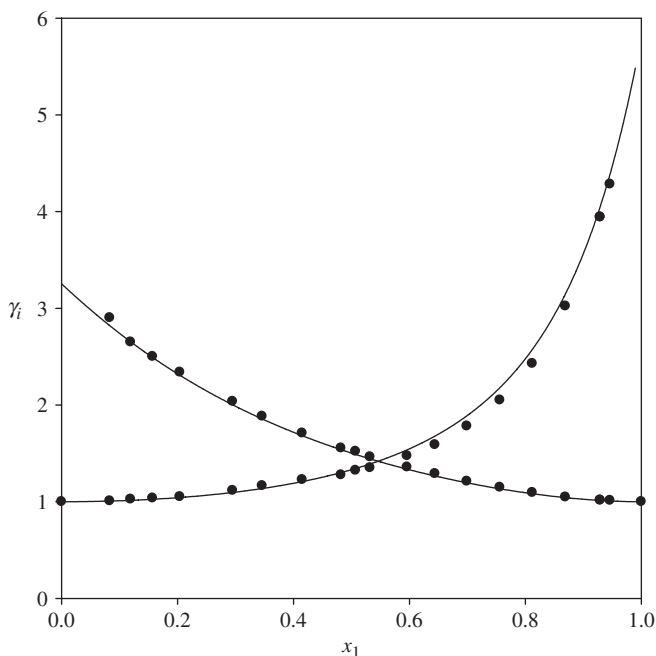


Figure 4. Activity coefficients for the system benzene (1) + propan-1-ol (2) at 94.00 kPa. (●) Experimental data; (—) smoothed by the NRTL model, with parameters given in table 8.

The standard state for calculation of activity coefficients is the pure component at the pressure and temperature of the solution. Equation (3) is valid from low to moderate pressures, when the virial equation of state truncated after the second coefficient is adequate to describe the vapor phase of the pure components and their mixtures, and liquid volumes of the pure components are incompressible over the pressure range under consideration. The molar virial coefficients B_{ii} , B_{jj} , and B_{ij} were estimated by the method of Hayden and O'Connell [72] using the molecular parameters suggested by the authors and assuming the association parameter η to be zero. B_{ii} , B_{jj} , and B_{ij} are reported in tables 2–4.

The temperature dependence of the pure component vapor pressure P_i^0 was calculated using the Antoine equation

$$\log\left(\frac{P_i^0}{\text{kPa}}\right) = A_i - \frac{B_i}{(T/\text{K}) - C_i} \quad (4)$$

where the Antoine constants A_i , B_i , and C_i are reported in table 5.

The calculated activity coefficients are reported in tables 2–4 and are estimated accurate to within $\pm 2\%$. The results reported in these tables indicate that, for the pressure range of the measurements, the liquid phase of the mixture benzene (1) + propan-1-ol (2) deviates positively from ideal behaviour and azeotropy is present at the three pressure levels. The azeotropic concentrations of the measured binaries were estimated by fitting the function

$$f(x) = 100\left(\frac{y-x}{x}\right) \quad (5)$$

Table 5. Antoine coefficients, (equation (4)).

Compound	A_i	B_i	C_i
Benzene ^a	6.0313	−1211.7511	−52.228
Propan-1-ol ^a	6.82728	−1414.0237	−77.032

^aMeasured.

Table 6. Estimated azeotropic coordinates for the system benzene (1) + propan-1-ol (2).

Pressure (kPa)	x_1^{Az}	T^{Az} (K)
50	0.824	329.56
75	0.800	340.76
94	0.785	347.38

Table 7. Consistency test statistics for the binary system benzene (1) + propan-1-ol (2).

Pressure (kPa)	N_p ^a	$100 \times \Delta y$ ^b	ΔP^c (kPa)
50.00	3	0.6	0.2
75.00	3	0.9	0.3
94.00	3	0.9	0.3

^aNumber of parameters for the Legendre polynomial used in consistency.^baverage absolute deviation in vapor phase mole fractions $\Delta y = (1/N) \sum_{i=1}^N |y_i^{\text{expt}} - y_i^{\text{cal}}|$ (N : number of data points).

where $f(x)$ is an empirical interpolating function and x , y have been taken from the experimental data. Azeotropic concentrations, as determined by solving $f(x) = 0$, are indicated in table 6, from which it is concluded that the mole fraction of the azeotrope impoverishes in benzene as pressure (or temperature) increases. The trend of the azeotropic concentration is in agreement with Wrewki's law [57], according to which a positive azeotrope becomes impoverished in the component characterized by the lowest heat of vaporization as pressure (or temperature) increases.

The VLE data reported in tables 2–4 were found to be thermodynamically consistent by the point-to-point method of Van Ness *et al.* [73] as modified by Fredenslund *et al.* [74] ($\Delta y < 0.01$). In all cases, consistency was met by fitting the data to a three parameter legendre polynomial. Pertinent consistency statistics are presented in table 7.

The present VLE data were also correlated with the Wohl, NRTL, Wilson, and UNIQUAC equations [75], whose parameters were obtained by minimizing the following objective function (OF):

$$\text{OF} = \sum_{i=1}^N \left(\frac{|P_i^{\text{exp}} - P_i^{\text{cal}}|}{P_i^{\text{exp}} + |y_i^{\text{exp}} - y_i^{\text{cal}}|} \right)^2 \quad (6)$$

The VLE data were also predicted using the UNIFAC [74,76] group contribution method. Pertinent parameters are reported in table 8, together with the relative deviation of the vapor phase mole fraction.

Table 8. Parameters and prediction statistics for different G^E models.

Model	P(kPa)	A ₁₂	A ₂₁	α ₁₂	Bubble-point pressures		Dew-point pressures	
					ΔP(%) ^f	100 × Δy _i	ΔP(%)	100 × Δx _i
Wohl	50.00	1.177	1.991	0.591 ^c	0.69	0.6	0.56	1.8
	75.00	1.163	1.815	0.752 ^c	0.41	0.7	0.86	1.9
	94.00	1.157	1.718	0.674 ^c	0.59	0.6	0.82	1.7
NRTL ^a	50.00	4756.63	1298.72	0.470	0.42	0.6	0.56	1.4
	75.00	4345.99	1335.60	0.470	0.52	0.7	0.83	1.6
	94.00	3978.25	1451.85	0.470	0.63	0.6	0.70	1.6
Wilson ^{a,b}	50.00	562.07	5868.10		0.44	0.5	0.53	1.1
	75.00	662.41	5305.81		0.68	0.6	0.89	1.4
	94.00	782.34	4876.01		0.73	0.6	0.76	1.4
UNIQUAC ^{a,c}	50.00	3094.59	-1072.28		0.36	0.5	0.49	1.1
	75.00	2743.84	-965.52		0.55	0.6	0.84	1.4
	94.00	2447.84	-844.96		0.67	0.6	0.72	1.5
UNIFAC ^d	50.00				4.20	2.3	2.96	5.2
	75.00				4.28	2.3	3.07	5.1
	94.00				3.88	2.4	2.66	5.0

^aParameters in J mol⁻¹. ^bLiquid volumes have been estimated from the Rackett equation [77]. ^cMolecular parameters are those calculated from UNIFAC [75]. ^dCalculations based on original UNIFAC [74,76]. ^e“*q*” Parameter for the Wohl’s model. ^fΔP = (100/N) ∑_i^N |P_i^{exp} - P_i^{cal}| / P_i^{exp}.

From the results presented in table 8, it is possible to deduce that all the fitted models gave a reasonable correlation of the binary systems, the best fit corresponding to the NRTL model. The capability of predicting simultaneously the vapor phase mole fraction and the equilibrium pressure has been used as the ranking factor. The deviation statistics reported in table 8 also show that the UNIFAC model [76] does not predict accurately the VLE data of the system reported in this work.

In order to compare our experimental results with the measurements by other authors, we predicted the VLE data reported by Brown and Smith at 318.15 K [34], and by Fu and Lu [35] 348.15 K using the parameters indicated in table 8. Results are shown in figure 5, where we can observe a very good agreement both in the predicted bubble-point (max ΔP = 3.10%, max Δy_i = 1.3%) and dew-point pressures (max ΔP = 1.88%, max Δx_i = 1.8%).

3.2. Excess volume data

The density of the mixture and its pure constituents at T = 298.15 K and P = 101.3 kPa are reported in table 9, together with the excess volumes V^E that were calculated from the following equation

$$V^E = \frac{1}{\rho} \sum_{i=1}^2 x_i M_i - \sum_{i=1}^2 x_i \frac{M_i}{\rho_i} \quad (7)$$

Where ρ is the density of the mixture, ρ_i is the density of the pure components, and M_i is the molecular weight of pure components whose values were taken from DIPPR [78]. The calculated excess volumes reported in table 9 are estimated accurate to within ±10⁻³ cm³ mol⁻¹.

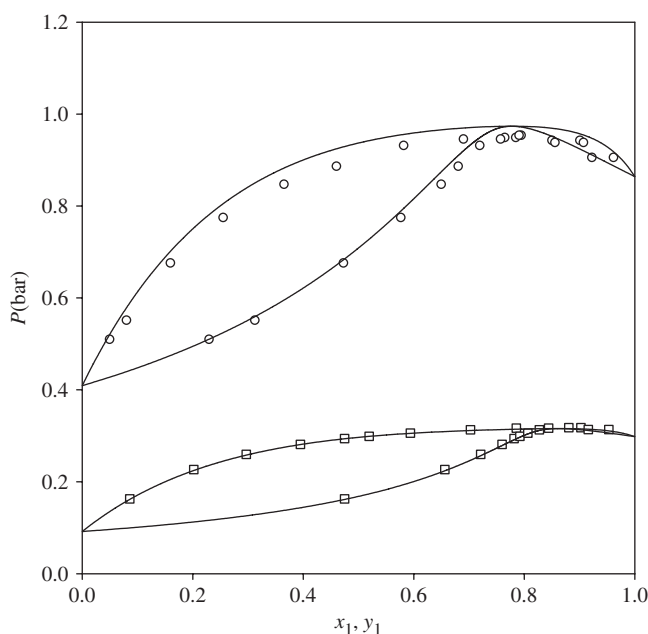


Figure 5. Isothermal phase diagram for the system benzene (1) + propan-1-ol (2). (—) Predicted from the NRTL model with the parameters indicated in table 8. (□) Experimental data at 318.15 K by Brown and Smith [34]. (○) Experimental data at 348.15 K by Fu and Lu [35].

Table 9. Densities and excess volumes for the binary system benzene (1) + propan-1-ol (2) at 298.15 K and 101.3 kPa.

x_1	ρ (g cm ⁻³)	$10^3 \times V^E$ (cm ³ mol ⁻¹)
0.0000	0.79948	0
0.0612	0.80488	-7
0.1717	0.81412	-1
0.2915	0.82351	26
0.3820	0.83027	54
0.4819	0.83748	85
0.5309	0.84090	102
0.5842	0.84460	115
0.6333	0.84798	125
0.6880	0.85170	134
0.7690	0.85719	136
0.8833	0.86496	112
0.9763	0.87155	44
1.0000	0.87346	0

Table 9 and figure 6 indicate that the sign of excess volumes of the system benzene (1) + propan-1-ol (2) changes from negative to positive as the concentration of benzene increases, behaviour that may be explained in terms of auto association of alkanol and the cross association between components, as expected for specific interactions between the polar alkanol and the benzene.

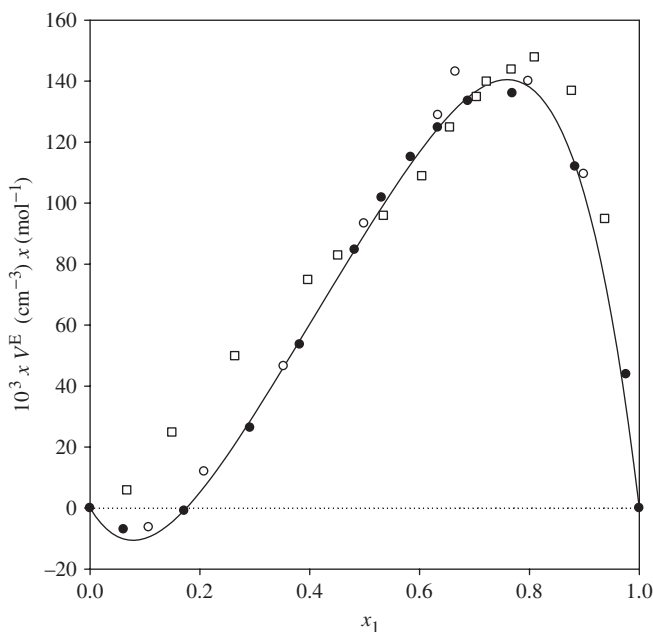


Figure 6. Excess volume for the system benzene (1)+propan-1-ol (2) at 298.15 K and 101.3 kPa. (●) Experimental data; (—) Smoothed by a Redlich–Kister expansion with the parameters shown in table 10. (○) Experimental data by Brown and Smith [59]. (□) Experimental data by Singh *et al.* [60].

Table 10. Coefficients in correlation of excess volumes, (equation (8)). Benzene (1) + propan-1-ol (2) at 298.15 K. Maximum, average, and SD.

c_0^a	c_1^a	c_2^a	c_3^a	$10^3(\text{cm}^3 \text{mol}^{-1})$		
				Max. dev.	Avg. dev.	SD
0.3593	-0.5746	0.2453	-0.3265	0.12	0.01	0.03

^aParameters in $\text{cm}^3 \text{mol}^{-1}$.

The excess volume data have been correlated using a three parameter Redlich–Kister expansion [79]

$$V^E = x_1 x_2 \sum_{k=0}^m c_k (x_1 - x_2)^k \quad (8)$$

where the c_k parameters, together with the correlation statistics, are reported in table 10.

Equation (8) was also used for predicting the V^E data reported by Brown and Smith [59] at 298.15 K. According to those results, a good agreement is obtained with maximum deviation of $0.15 \times 10^{-3} \text{cm}^3 \text{mol}^{-1}$ (figure 6). In this figure, we also included the values reported by Singh *et al.* [60], and we observe that at benzene mole fraction lower than 0.4 these results differ, significantly, from our results and the data measured

from Brown and Smith. A possible explanation for this difference may be attributed to the accuracy of the dilatometric technique used by Singh *et al.*

3.3. Interfacial tension data

The interfacial tension measurements at $T = 298.15$ K and $P = 101.3$ kPa are reported in table 11 and depicted in figure 7.

These experimental data were also correlated using the following Redlich–Kister expansion [80]

$$\sigma = x_1 x_2 \sum_{k=0}^m c_k (x_1 - x_2)^k + x_1 \sigma_1 + x_2 \sigma_2 \quad (9)$$

Table 11. Interfacial tensions for the binary system benzene (1) + propan-1-ol (2) at 298.15 K and 101.3 kPa.

x_1	σ (mN m ⁻¹)
0.000	23.50
0.198	24.10
0.316	24.60
0.455	25.15
0.595	25.80
0.738	26.45
0.878	27.25
1.000	28.30

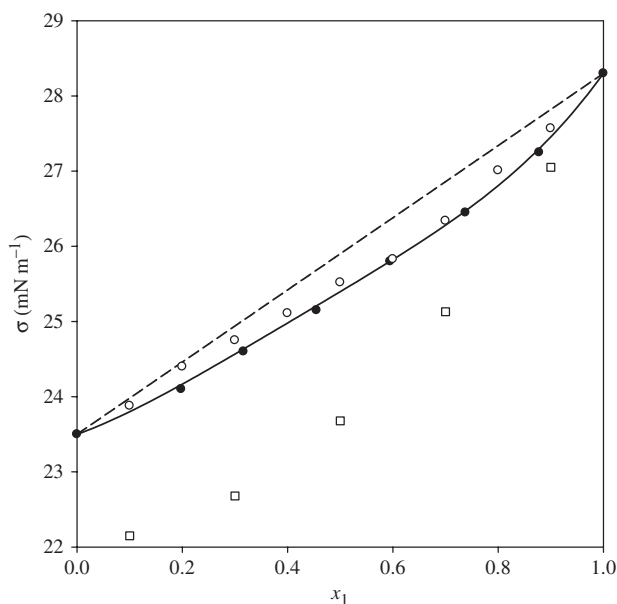


Figure 7. Interfacial tension for the system benzene (1) + propan-1-ol (2) at 298.15 K and 101.3 kPa. (●) Experimental data; (—) smoothed by a Redlich–Kister expansion with the parameters shown in table 12. (---) Linear behaviour, (○) experimental data by Starobinets and Starobinets [65], (□) experimental data by Shastri *et al.* [66].

Table 12. Coefficients in correlation of interfacial tension, (equation (9)), benzene (1) + propan-1-ol (2) at 298.15 K. Maximum, average, and SD.

c_0^a	c_1^a	c_2^a	$10^3(\text{mN m}^{-1})$		
			Max. dev.	Avg. dev.	SD
-2.1326	1.0762	-2.0559	0.63	0.23	0.27

^aParameters in mN m^{-1} .

In equation (9), σ is the interfacial tension of the mixture while σ_i is the interfacial tension of the pure components. The c_k parameters of equation (9), together with the correlation statistics, are reported in table 12.

From figure 7 it is possible to observe that the interfacial tensions of the mixture benzene + propan-1-ol exhibit negative deviation from the lineal behaviour ($x_1\sigma_1 + x_2\sigma_2$). In addition, it is possible to observe that the interfacial tension of the mixture increase as the benzene concentration increases.

Equation (9) was also used for predicting the σ data reported by Starobinets and Starobinets [65], and Shastri *et al.* [66] at 298.15 K. Comparing these results (figure 7), we obtain a good agreement with Starobinets and Starobinets values (a maximum difference of 0.09 mN m^{-1}) and a fair agreement is with Shastri *et al.* (a maximum difference of 3.7 mN m^{-1}).

4. Concluding remarks

In this work, consistent isobaric VLE data (at 50, 75, and 94 kPa), excess molar volumes and interfacial tension data at 298.15 K were measured for the system benzene + propan-1-ol. The system exhibits positive deviation from ideal behaviour and azeotropic behaviour is present at 50, 75, and 94 kPa. At lower pressures, and in coherency with the data reported by Brown and Smith and Fu and Lu the azeotrope follows Wrewki's law. The excess volume of the system changes from negative to positive as the concentration of benzene increases. These results are in good agreement with the data reported by Brown and Smith [59]. The interfacial tensions of the system exhibits negative deviation from the lineal behaviour, and our results show a very good agreement with the measurement from Starobinets and Starobinets [65]. The activity coefficients and boiling points of the solutions were well correlated with the mole fraction using the Wohl, Wilson, UNIQUAC, NRTL equations; whose parameters also predicted the data reported by Brown and Smith and Fu and Lu. Excess volume data and interfacial tensions were correlated using the Redlich–Kister expansion. These correlations also predicted the data reported by Brown and Smith [59] and Starobinets and Starobinets [65], respectively.

Acknowledgment

This work was financed by FONDECYT, Santiago, Chile (Project 1050157).

References

- [1] M.C. Burguet, J.B. Monton, R. Muñoz, J. Wisniak, H. Segura. *J. Chem. Eng. Data*, **41**, 1191 (1996).
- [2] J. Wisniak, E. Magen, M. Shachar, I. Zeroni, R. Reich, H. Segura. *J. Chem. Eng. Data*, **42**, 243 (1997).
- [3] J. Wisniak, E. Magen, M. Shachar, I. Zeroni, R. Reich, H. Segura. *J. Chem. Eng. Data*, **42**, 458 (1997).
- [4] A. Aucejo, S. Loras, R. Muñoz, J. Wisniak, H. Segura. *J. Chem. Eng. Data*, **42**, 1201 (1997).
- [5] J.B. Montón, M.C. Burguet, R. Muñoz, J. Wisniak, H. Segura. *J. Chem. Eng. Data*, **42**, 1195 (1997).
- [6] J. Wisniak, G. Embon, R. Shafir, H. Segura, R. Reich. *J. Chem. Eng. Data*, **42**, 1191 (1997).
- [7] R. Reich, M. Cartes, J. Wisniak, H. Segura. *J. Chem. Eng. Data*, **43**, 299 (1998).
- [8] J. Wisniak, E. Fishman, R. Shaulitch, R. Reich, H. Segura. *J. Chem. Eng. Data*, **43**, 307 (1998).
- [9] A. Aucejo, S. Loras, R. Muñoz, R. Reich, H. Segura. *J. Chem. Eng. Data*, **43**, 973 (1998).
- [10] J. Wisniak, G. Embon, R. Shafir, R. Reich, H. Segura. *Phys. Chem. Liq.*, **37**, 51 (1998).
- [11] J. Wisniak, G. Galindo, R. Reich, H. Segura. *Phys. Chem. Liq.*, **37**, 649 (1999).
- [12] R. Reich, M. Cartes, J. Wisniak, H. Segura. *Fluid Phase Equilib.*, **154**, 99 (1999).
- [13] J. Wisniak, R. Reich, H. Segura. *Fluid Phase Equilib.*, **154**, 213 (1999).
- [14] H. Segura, R. Reich, G. Galindo, J. Wisniak. *J. Chem. Eng. Data*, **44**, 912 (1999).
- [15] R. Reich, M. Cartes, H. Segura, J. Wisniak. *Phys. Chem. Liq.*, **38**, 73 (2000).
- [16] H. Segura, G. Galindo, J. Wisniak, R. Reich. *Phys. Chem. Liq.*, **38**, 391 (2000).
- [17] R. Reich, M. Cartes, H. Segura, J. Wisniak. *Phys. Chem. Liq.*, **38**, 218 (2000).
- [18] H. Segura, R. Reich, G. Galindo, J. Wisniak. *J. Chem. Eng. Data*, **45**, 600 (2000).
- [19] J. Wisniak, H. Segura. *Phys. Chem. Liq.*, **38**, 553 (2000).
- [20] H. Segura, E. Lam, R. Reich, J. Wisniak. *Phys. Chem. Liq.*, **39**, 43 (2001).
- [21] J. Wisniak, B. Yarden, T. Sling, H. Segura. *J. Chem. Eng. Data*, **46**, 223 (2001).
- [22] H. Segura, R. Reich, G. Galindo, J. Wisniak. *J. Chem. Eng. Data*, **46**, 506 (2001).
- [23] H. Segura, J. Wisniak, G. Galindo, R. Reich. *J. Chem. Eng. Data*, **46**, 511 (2001).
- [24] H. Segura, R. Reich, G. Galindo, J. Wisniak. *Phys. Chem. Liq.*, **39**, 637 (2001).
- [25] S. Loras, A. Aucejo, J.B. Montón, J. Wisniak, H. Segura. *J. Chem. Eng. Data*, **46**, 1351 (2001).
- [26] S. Loras, A. Aucejo, J.B. Montón, J. Wisniak, H. Segura. *J. Chem. Eng. Data*, **47**, 1256 (2002).
- [27] H. Segura, G. Galindo, R. Reich, J. Wisniak, S. Loras. *Phys. Chem. Liq.*, **40**, 277 (2002).
- [28] H. Segura, J. Wisniak, R. Reich, G. Galindo. *Phys. Chem. Liq.*, **40**, 67 (2002).
- [29] H. Segura, A. Mejía, R. Reich, J. Wisniak, S. Loras. *Phys. Chem. Liq.*, **40**, 685 (2002).
- [30] H. Segura, A. Mejía, R. Reich, J. Wisniak, S. Loras. *Phys. Chem. Liq.*, **41**, 283 (2003).
- [31] H. Segura, A. Mejía, R. Reich, J. Wisniak, S. Loras. *Phys. Chem. Liq.*, **41**, 493 (2003).
- [32] G.C. Schmidt. *Z. Phys. Chem. Stoehiom. Verwandtschaftsl.*, **121**, 221 (1926).
- [33] S.C. Lee. *J. Phys. Chem.*, **35**, 3558 (1931).
- [34] I. Brown, F. Smith. *Aust. J. Chem.*, **12**, 407 (1959).
- [35] J.M. Skaates, W.B. Kay. *Chem. Eng. Sci.*, **19**, 431 (1964).
- [36] S.J. Fu, B.C.Y. Lu. *J. Appl. Chem.*, **16**, 324 (1966).
- [37] V.V. Udovenko, T.F. Mazanko. *Izv. Vyssh. Uchebn. Zaved. Khim. Khim. Tekhnol.*, **15**, 1654 (1972).
- [38] K. Strubl, V. Svoboda, R. Holub, J. Pick. *Collect. Czech. Chem. Commun.*, **40**, 1647 (1975).
- [39] A. Arce, A. Blanco, G. Antorrena. *Acta Cient. Compostelana*, **14**, 145 (1977).
- [40] S.C. Hwang, R.L. Robinson. *J. Chem. Eng. Data*, **22**, 319 (1977).
- [41] P. Oracz, G. Kolasinska. *Fluid Phase Equilib.*, **35**, 253 (1987).
- [42] V. Gupta, S. Maken, K.C. Kalra, K.C. Singh. *Thermochim. Acta.*, **277**, 187 (1996).
- [43] K. Kurihara, M. Uchiyama, K. Kojima. *J. Chem. Eng. Data*, **42**, 149 (1997).
- [44] S. Maken, V. Gupta, K. Kalra, K.C. Singh. *Indian J. Chem. Sect. A*, **38**, 219 (1999).
- [45] J.M. Rhodes, T.A. Griffin, M.J. Lazzaroni, V.R. Bhethanabotla, S.W. Campbell. *Fluid Phase Equilib.*, **179**, 217 (2001).
- [46] E.C. Britton, H.S. Nutting, L.H. Horsley. *Anal. Chem.*, **8**, 601 (1947).
- [47] E. Bonauguri, L. Bicelli, G. Spiller. *Chim. Ind. Milan.*, **33**, 81 (1951).
- [48] A.H. Wehe, J. Coates. *J. AIChE*, **1**, 241 (1955).
- [49] A.G. Morachevskii, C.T. Chen. *Russ. J. Phys. Chem.*, **10**, 1153 (1961).
- [50] P.S. Prabhu, M. van Winkle. *J. Chem. Eng. Data*, **8**, 210 (1963).
- [51] V.V. Udovenko, T.F. Mazanko, V. Ya Plyngeu. *Zh. Fiz. Khim.*, **1**, 218 (1972).
- [52] G. Tojo Barreiro, M. Bao, A. Arce. *An. Quim.*, **11**, 1177 (1973).
- [53] J.L. Cabezas, J.C. Arranz, J. Berruela. *J. Rev. Roum. Chim.*, **6**, 903 (1985).
- [54] T. Hiaki, K. Tochigi, K. Kojima. *Fluid Phase Equilib.*, **26**, 83 (1986).
- [55] V.Yu. Aristovich, A.S. Dovedova, V.N. Kiva, Yu.A. Tsirlin, Tr. Vnii Gidroliza Rastitel N. *Materialov.*, **10**, 59 (1981).
- [56] W. Shouyu, Z. Chenpu. *Huagong Xuebao.*, **2**, 72 (1991).
- [57] W. Malesinski. *Azeotropy and other Theoretical Problems of Vapour–Liquid Equilibrium*, Interscience Publishers, London (1965).
- [58] P. Munk, A. Qin, D.E. Hoffmann. *Collect. Czech. Chem. Commun.*, **11**, 2612 (1993).

- [59] I. Brown, F. Smith. *Aust. J. Chem.*, **15**, 1 (1962).
- [60] K.C. Singh, K.C. Kalra, S.Y. Maken, B.L. Yadav. *J. Chem. Eng. Data*, **39**, 241 (1994).
- [61] V. Gupta, S. Maken, K.C. Kalra, K.C. Singh. *Indian J. Chem. Sect. A*, **6**, 508 (1996).
- [62] K.S. Kumar, N.V. Reddy. *Phys. Chem. Liq.*, **39**, 117 (2001).
- [63] B.L. Yadav, S. Maken, K.C. Kalra, K.C. Singh. *J. Chem. Thermodyn.*, **25**, 1345 (1993).
- [64] A.S. Brown. *Zh. Obshch. Khim.*, **3**, 973 (1933).
- [65] G.L. Starobinets, K.S. Starobinets. *Zh. Fiz. Khim.*, **25**, 753 (1951).
- [66] S.S. Shastri, A.K. Mukherjee, T.R. Das. *J. Chem. Eng. Data*, **38**, 399 (1993).
- [67] J.A. Riddick, W.B. Bunger, T.K. Sakano. *Organic Solvents. Techniques of Chemistry*, 4th Edn, Vol. II, Wiley, New York (1986).
- [68] J.J. Jasper. *J. Phys. Chem. Ref. Data*, **1**, 841 (1972).
- [69] A.W. Adamson, A.P. Gast. *Physical Chemistry of Surfaces*, Wiley Interscience, USA (1997).
- [70] A.I. Rusanov, V.A. Prokhorov. *Interfacial Tensiometry*, Elsevier, Netherlands (1996).
- [71] H.C. Van Ness, M.M. Abbott. *Classical Thermodynamics of Nonelectrolyte Solutions*, McGraw-Hill Book Co., New York (1982).
- [72] J. Hayden, J.A. O'Connell. *Ind. Eng. Chem. Process Des. Dev.*, **14**, 209 (1975).
- [73] H.C. Van Ness, S.M. Byer, R.E. Gibbs. *AIChE J*, **19**, 238 (1973).
- [74] Aa. Fredenslund, J. Gmehling, P. Rasmussen. *Vapor-Liquid Equilibria Using UNIFAC*, Elsevier, Amsterdam (1977).
- [75] J.M. Prausnitz, R.N. Lichtenthaler, E. Gomes de Azevedo. *Molecular Thermodynamics of Fluid-Phase Equilibria*, 3th Edn, Prentice Hall, New Jersey (1999).
- [76] H.K. Hansen, P. Rasmussen, Aa. Fredenslund. *Ind. Eng. Chem. Res.*, **30**, 2352 (1991).
- [77] H.G. Rackett. *J. Chem. Eng. Data*, **15**, 514 (1970).
- [78] T.E. Daubert, R.P. Danner. *Physical and Thermodynamic Properties of Pure Chemicals. Data Compilation*, Taylor and Francis, Bristol, PA (1989).
- [79] O. Redlich, A.T. Kister. *Ind. Eng. Chem.*, **40**, 341 (1948).
- [80] D.B. Myers, R.L. Scott. *Ind. Eng. Chem.*, **55**, 43 (1963).